ISBN: 978-3-95450-234-9 ISSN: 2673-5504 doi:10.18429/JACoW-SRF2023-MOPMB022

RECENT MID-T SINGLE-CELL TREATMENTS R&D AT DESY*

C. Bate†, D. Reschke, J. Schaffran, L. Steder, L. Trelle, H. Weise
Deutsches Elektronen-Synchrotron DESY, Hamburg, Germany

Abstract

The challenge of improving the performance of SRF cavities is being faced worldwide. One approach is to modify the superconducting surface properties through certain baking procedures. Recently a niobium retort furnace placed directly under an ISO4 clean room has been refurbished at DESY. Thanks to an inter-vacuum chamber and cryopumps, with high purity values in the mass spectrum it is working in the UHV range of 2×10^{-8} mbar. The medium temperature (mid-T) heat treatments around 300 °C are promising and successfully deliver reproducible very high Q_0 values of $2-5\times10^{10}$ at medium field strengths of 16 MV/m. Since the first DESY and Zanon Research & Innovation Srl (Zanon) mid-T campaign yielded promising results, further results of 1.3 GHz single-cell cavities are presented here after several modified treatments of the mid-T recipe.

In addition, samples were added to each treatment, the RRR value change was examined, and surface analyses were subsequently performed. The main focus of the sample study is the precise role of the changes in the concentration of impurities on the surface. In particular, the change in oxygen content due to diffusion processes is suspected to be the cause of enhancing the performance.

MID-T HEAT TREATMENTS AT DESY

In-situ medium temperature bake experiments conducted at approximately 300 °C [1] demonstrated remarkable high quality-factors. Subsequently, two studies [2, 3] performed mid-T heat treatments using commercially available ultra-high vacuum (UHV) furnaces, followed by sequential cleaning and assembly procedures of the cavities in an air environment. DESY has also investigated this treatment as part of its R&D programs, which was presented in Ref. [4]. This approach shows great potential for future applications in accelerator projects. The performance characteristics of the cavities, as depicted by the quality factor Q_0 versus the accelerating gradient E_{acc} (Q(E)), closely resemble those observed for nitrogen-doped cavities [5,6]. Notably, there is an increase in Q_0, reaching its peak at an E_{acc} of approximately 16 MV/m, commonly called the "anti-Q-slope." Further investigation is required to determine whether the mid-T heat treatment exhibits comparable limitations on the gradient, similar to specific doping techniques [5, 7], or whether it can provide high gradients surpassing 30 MV/m. A major advantage of the mid-T heat treatment approach compared to other recipes that achieve similar performances is its significantly shorter baking time and absence of the need for additional gases such as nitrogen in the furnace. In addition, no chemical surface treatment is required afterwards.

NIOBIUM-RETORT FURNACE

In late 2021, the newly refurbished all-niobium furnace at DESY enabled the application of heat treatments. The furnace, located in the ISO 4 area of the cavity assembly clean room, comprises a niobium retort with a separate vacuum enclosure that houses the heaters. It has a usable diameter of 0.3 m and a depth of 1.3 m, allowing for the treatment of a 1.3 GHz nine-cell cavity or one or two single-cell cavities simultaneously, all positioned vertically as depicted in Fig. 1. The heat ramping of the furnace is regulated by temperature sensors located near the heating zone outside of the separate vacuum. Additional temperature sensors installed near the cavity equators on the insert are monitored and utilized for analysis. The furnace can reach a maximum temperature of

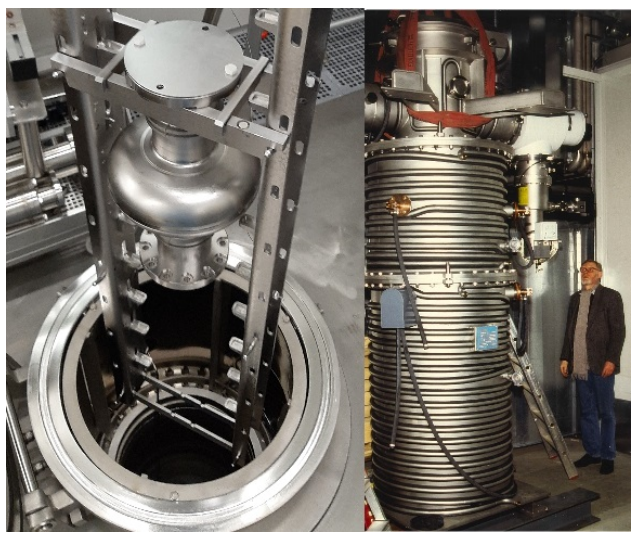

Figure 1: Single-cell Cavity inserted in the niobium-retort furnace (left side). External view of the niobium retort furnace during the initial assembly at DESY (right side).

1200 °C. The complete refurbishment involved the renewal of the entire vacuum, cooling, and control system, as well as the implementation of partial pressure control and a mass spectrometry system. The cryo pumping system is oil-free and maintains a base pressure of 2×10^{-8} mbar at room temperature. During cavity treatment at 800 °C, the pressure steadily increases to approximately $3 - 4 \times 10^{-7}$ mbar. After the furnace qualification, two successful treatments were conducted at 800 °C. While the commissioning of the furnace is complete, ongoing efforts focus on improving control features and establishing reproducible treatment protocols. Additionally, it is planned to conduct a tandem run,

* This work was supported by the Helmholtz Association within the topic Accelerator Research and Development (ARD) of the Matter and Technologies (MT) Program.
† christopher.bate@desy.de

Content from this work may be used under the terms of the CC BY 4.0 licence (© 2023). Any distribution of this work must maintain attribution to the author(s), title of the work, publisher, and DOI

ISBN: 978-3-95450-234-9 ISSN: 2673-5504 doi:10.18429/JACoW-SRF2023-MOPMB022

Content from this work may be used under the terms of the CC BY 4.0 licence (© 2023). Any distribution of this work must maintain attribution to the author(s), title of the work, publisher, and DOI

treating two single-cell cavities simultaneously and treating a nine-cell cavity, to further expand the scope of the investigation with the goal of establishing recipes for industrial application. Further comprehensive information regarding the furnace, including detailed specifications and operational procedures, can be found in Ref. [8].

MID-T CAMPAIGN

After the furnace commissioning, mid-T treatments on three 1.3 GHz single-cell cavities were performed to investigate the impact of the diffusion length of interstitial oxygen from the niobium oxide layers at the surface into the bulk [4]. In total mid-T treatments on seven fine-grain cavities and one large-grain (LG) cavity have been performed, each employing varied parameters, bringing the total number of mid-T treatments at DESY to eight. The results from these additional treatments form the main focus of the findings presented in this study. The temperatures and durations were changed from 250 °C to 300 °C and from 3 to 20 hours. In contrast to the standard procedure at DESY, where always a "low-T" bake after the final electropolishing (EP) step is applied, it was omitted for these cavities. This decision was based on the understanding that the low-T treatment affects the oxygen distribution in niobium. Previous research [4] has shown that the low-T bake is not necessary prior to a mid-T treatment and will reduce the time and effort for cavity preparation.

Q_0 *Versus* E_{acc}

The characteristic features of mid-T treated cavities were observed and confirmed several times as shown in Fig. 2, where Q(E)-curves measured at 2 K for all treatments are shown. Of those eight measurements shown, four experienced a drop in Q_0 after quenching. Note that the estimated uncertainty of independent rf measurements (test to test) is approximately ~10% for E_{acc} and up to ~20% for Q_0. However, within a single cold vertical test (e.g., the comparison between filled and empty markers before and after quenching in Fig. 2) and for each Q_0(E) curve, the observed measurement scatter is significantly smaller, at around 1% for E and 3% for Q_0 [9]. Clearly, there appears to be an apparent barrier for the maximum accelerating gradients at 30 MV/m, the underlying cause of which is currently under investigation in the most recent research. Both cavities 1DE7 and 1RI2, treated for 20 hours at 250 °C, exhibit the characteristic anti-Q slope, but the overall improvement in Q_0 is less significant compared to the cavities treated at 300 °C or for shorter durations. The performance of 1DE17, which was also subjected to a 20-hour treatment at 300 °C and exhibited good performance, indicates that the duration of 20 hours alone does not appear to be the determining factor.

Approximated R_{BCS}

Using Q(E)-curves acquired at 2 K and 1.5 K, and considering the negligible temperature-dependent contribution to the surface resistance R_S at 1.5 K (usually ≤ 1 nΩ), a measure closely approximating $R_{BCS} \approx R_{S,2K} - R_{S,1.5K}$ at 2 K was deduced and is presented in Fig. 3. For medium gradients around 16 MV/m, the estimated R_{BCS} ranges from 4 to 6 nΩ after all mid-T treatments, which is significantly lower than the R_{BCS} for the baseline test following electropolishing (9-12 nΩ). Even lower R_{BCS} of about 3 nΩ were shown in Ref. [4]. Additionally, a distinct concave curvature is observed, leading to the characteristic anti-Q-slope. These findings hold true even for mid-T treatments, such as 1DE7 or 1RI2, which exhibited less favourable measures of E_{acc} and Q_0 at 2 K. Similar performance characteristics have also been observed in previous studies [3] for mid-T treatments, as well as in N-doped cavities [10], indicating that impurities such as nitrogen and oxygen have a comparable impact on cavity performance.

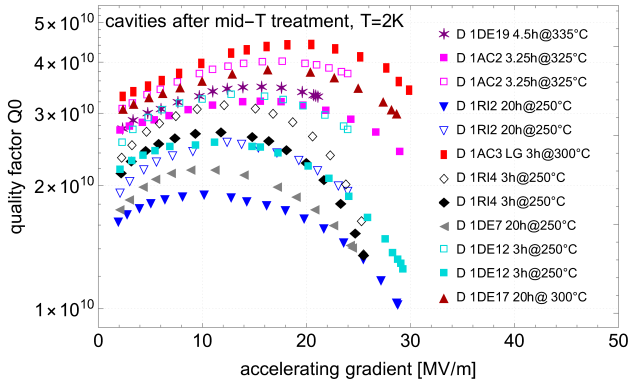

Figure 2: Q(E) for all mid-T heat treatments. The temperature and duration of each treatment are indicated. The filled symbols represent the final status of the respective vertical tests, including the maximum gradient achieved. The additional curves with empty markers were obtained to investigate the maximum Q_0 and were deliberately terminated before the cavities experienced quenching. 1AC3 is a large-grain (LG) cavity.

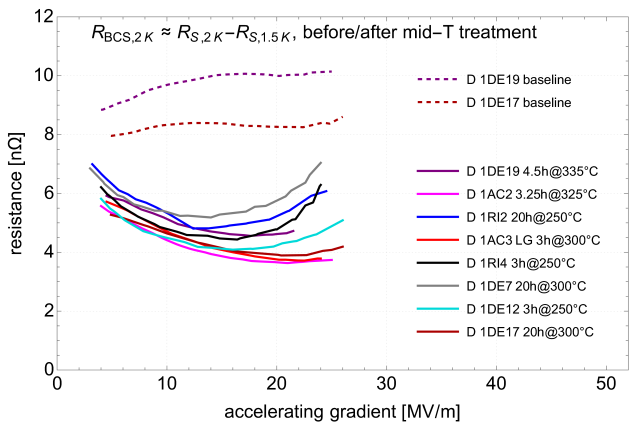

Figure 3: Estimation of R_{BCS} for all mid-T heat treatments, along with corresponding baseline measurements (dashed). 1AC3 is a large-grain (LG) cavity.

ISBN: 978-3-95450-234-9 ISSN: 2673-5504 doi:10.18429/JACoW-SRF2023-MOPMB022

Correlation to the Oxygen Diffusion Length

Speculations, about why simply baking a cavity in a vacuum for certain temperatures and durations have such a pronounced effect on the Q(E) performance, have been attributed to interstitial oxygen for a long time. It has been demonstrated that the oxide layer on the surface of niobium undergoes decomposition within the temperature range of 200 °C to 300 °C [11–13].

In order to account for the cumulative effect of temperature on diffusion length, which is dependent on the thermal characteristics of the furnace, the diffusion coefficient was calculated by integrating the temperature ramp over time.

The Arrhenius equation

$$D(T) = D_0 \cdot e^{-\frac{E_a}{kT}}, \quad (1)$$

describes the temperature-dependent diffusion coefficient for oxygen atoms in Nb, where $D_0 = 0.015\ \frac{\mathrm{cm}^2}{\mathrm{s}}$ represents the diffusion constant, $E_a = 1.2\,\mathrm{eV}$ denotes the activation energy [14], and k refers to the Boltzmann constant. These parameters, D_0 and E_a, are commonly referred to as diffusion activation parameters.

By applying Fick's Law [15] to Eq. (1), we can determine the diffusion length from the surface as $l = 2\sqrt{Dt}$ where t is the time. Since the objective is to consider the entire heat ramp of the furnace run, the diffusion coefficient becomes time-dependent due to the varying temperature. To account for this, numerical integration of the diffusion coefficient over time $l = 2\sqrt{\int D(t)dt}$ is performed, utilizing data from the temperature sensor closest to the cavity equators (see Ref. [8] for more details on sensor positions). The temperature data provides insights into the thermal history, allowing us to estimate the oxygen diffusion behaviour during the heat treatments. Figure 4 presents the temperature profiles over time for each mid-T heat treatment, along with the corresponding oxygen diffusion lengths indicated in the legend. The diffusion lengths are calculated using the integrated area of the temperature curves, as shown in the small inset figure.

The maximum achieved quality factor at 2 K for each cavity is depicted against the oxygen diffusion length in Fig. 5. It should be noted that 1AC3, being an LG cavity does not represent the same conditions as the other cavities and is included for comparison purposes. Considering only the cavities of the same kind, a linear behaviour is observed, suggesting a possible upward trend. However, due to the limited precision and small sample size, statistical accuracy to confirm this trend is lacking. It is notable how the treatments with similar diffusion lengths cluster together, as observed, in the case of 1RI4 along with 1DE12 and 1RI2 along with 1DE7, which is consistent with the comparison to the oxygen diffusion length thus far. Further measurements will be conducted to confirm this.

Figure 6 depicts the plotted relationship between the approximated R_{BCS} value at 2 K and 16 MV/m from each cavity and the corresponding diffusion length. No discernible specific pattern is evident; however, it is noteworthy that

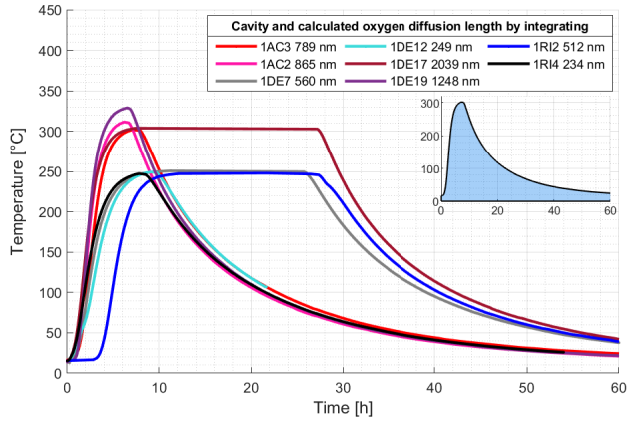

Figure 4: Temperature profiles of each mid-T heat treatment. The corresponding oxygen diffusion length is indicated in the legend. Shown as a small inset on the right is the numerically integrated area of one temperature profile, used to determine the diffusion length.

the cluster of 1RI4 along with 1DE12 and 1RI2 along with 1DE7 remains consistent. In summary, these observations indicate a tendency for increasing Q_0 values with longer oxygen diffusion lengths. However, the data lacks sufficient precision to firmly establish this relationship.

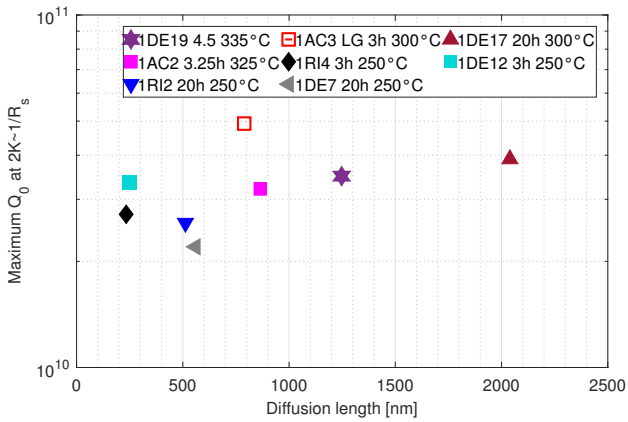

Figure 5: Maximum Q_0 value for all mid-T heat treatments against diffusion length. 1AC3 is an LG cavity (highlighted by empty markers).

SAMPLES

The DESY treatments were conducted concurrently using two types of niobium samples. The first type (cylindrical ⌀ 12 mm) underwent electropolishing (before and after 800 °C baking for 3 hours) immediately prior to the furnace runs, specifically for surface analysis techniques such as secondary ion mass spectrometry (SIMS). The second type of samples underwent buffered chemical polishing (BCP) prior to the furnace runs, primarily for measuring the residual resistivity ratio (RRR). Due to the sample geometry (2.8 x 3 x 40) mm, electropolishing was not undertaken. For further details

Content from this work may be used under the terms of the CC BY 4.0 licence (© 2023). Any distribution of this work must maintain attribution to the author(s), title of the work, publisher, and DOI

ISBN: 978-3-95450-234-9 ISSN: 2673-5504 doi:10.18429/JACoW-SRF2023-MOPMB022

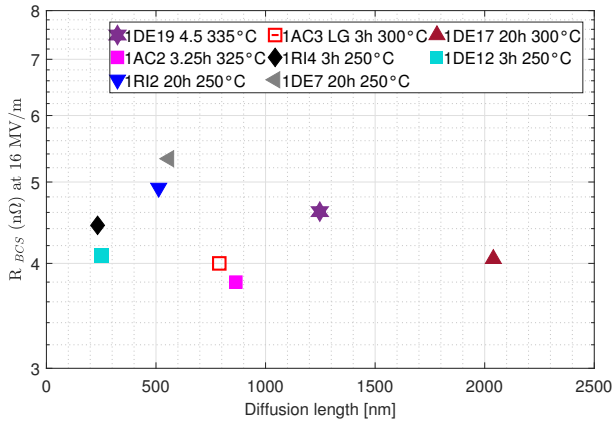

Figure 6: $R_{BCS,2K} \approx R_{S,2K} - R_{S,1.5K}$ for all mid-T heat treatments against diffusion length. AC3 is an LG cavity (highlighted with empty markers).

regarding the RRR samples and measurement setup, refer to Ref. [16].

RRR Results

The Residual Resistivity Ratio (RRR) is defined as the ratio of the electrical resistance, ρ(T), at room temperature (295 K) to the residual resistance at 4.2 K

$$\mathrm{RRR} = \rho(295\,\mathrm{K})/\rho(4.2\,\mathrm{K}). \quad (2)$$

A higher RRR value indicates a lower presence of defects and interstitials within the material. Therefore, RRR serves as an indicator of the purity of a metal. It is highly responsive to changes in impurity levels caused by diffusion during various treatments, such as heat treatments in vacuum or under specific gas atmospheres, or chemical surface treatments.

The difference in RRR between before and after the treatment denoted as ΔRRR is shown in Table 1 for each mid-T treatment which was accompanied by a RRR sample.

The only treatment that significantly deteriorated the RRR by a factor of about 4% is the 300 °C treatment applied for 20 hours (negative value for ΔRRR). Unfortunately, the measurement accuracy was not sufficient to make further significant conclusions between the treatments. However, there are plans to repeat these measurements using thin samples with thicknesses ranging from 300-900 µm. Thin samples offer a larger surface-to-bulk ratio, which can provide more comprehensive insights into the phenomenon.

SIMS Results

The plots in Fig. 7 present normalized profiles obtained from Secondary Ion Mass Spectrometry (SIMS) analyses. Figures (a)-(c) depict near-surface profiles up to a depth of 40 nm, while (d)-(f) display the overall profiles obtained. We aimed to obtain profiles at depths corresponding to the calculated diffusion lengths. The calculated diffusion lengths are 1248 nm for 1DE19, 865 nm for 1AC2, and 512 nm for 1RI02. However, measurements of the crater depths revealed the sputtering lasted just slightly above 250 nm. Interestingly, for sample 218, which underwent treatment at 250 °C for 20 hours along with 1RI2 and has the smallest diffusion length, the oxygen profile exhibits a gradual decrease starting at approximately 210 nm, as illustrated by the NbO_2^+ signal in figure (f). However, the observed profile deviates from the expected concentration profile based on Fick's law. No significant differences were observed in the near-surface profiles of negative ion recombinations, and therefore, they are not presented in this study. Only the positive signals, such as NbO^+ and NbO_2^+, revealed distinct disparities between the 250 °C and >300 °C treatments. Additionally, a slight difference was observed in NbO_2^+ and CNb^+ between the 335 °C treatment for 4.5 hours and the 325 °C treatment for 3.25 hours. No other measured ion recombinations provided further information on the diffusion processes and are therefore not presented.

Table 1: Comparison of RRR (at 4.2 K) Values Measured on Fine Grain Samples (RRR ~ 300) before and after a Mid-T Heat Treatment, Along with a Cavity

Cavity	Anneal time	Before	After	ΔRRR
1DE18	3 h 300 °C	347	355	9±8
1DE18	3 h 300 °C	339	340	1±8
1DE26	3 h 300 °C	312	315	3±7
1DE17	20 h 300 °C	355	343	-12±7
1RI04	3 h 250 °C	358	373	15±8
1DE12	3 h 250 °C	343	355	12±7
1DE7	20 h 250 °C	338	356	18±7

SUMMARY AND CONCLUSION

All mid-T heat treated cavities exhibit distinct Q(E) curves and a reduced R_{BCS}, with the majority displaying high Q_0 values and gradients of approximately 30 MV/m. However, no indication of how this apparent barrier of 30 MV/m can be broken through in the accelerator gradient has yet been found. These findings reinforce the results obtained in the initial mid-T heat treatment campaign at DESY and are further substantiated by the additional data presented in this study. The observed correlations between cavity performance and oxygen diffusion length suggest a tendency of increasing Q_0 values with longer diffusion lengths. However, the available data lack the required precision to establish this relationship definitively. Significant differences in oxygen concentrations between mid-T heat treatments at 300 °C and 250 °C are revealed through SIMS studies. Additionally, the RRR studies demonstrate a clear distinction between the 300 °C treatment applied for 20 hours and the other temperature conditions. Furthermore, thinner samples are being prepared for RRR measurements to increase the surface-to-bulk ratio and enhance the notable surface effect through the redistribution of oxygen impurities.

As the results demonstrate, the low-T bake and any additional electropolishing step are unnecessary and eliminate a time-consuming processing step in the overall procedure of

Content from this work may be used under the terms of the CC BY 4.0 licence (© 2023). Any distribution of this work must maintain attribution to the author(s), title of the work, publisher, and DOI

ISBN: 978-3-95450-234-9 ISSN: 2673-5504 doi:10.18429/JACoW-SRF2023-MOPMB022

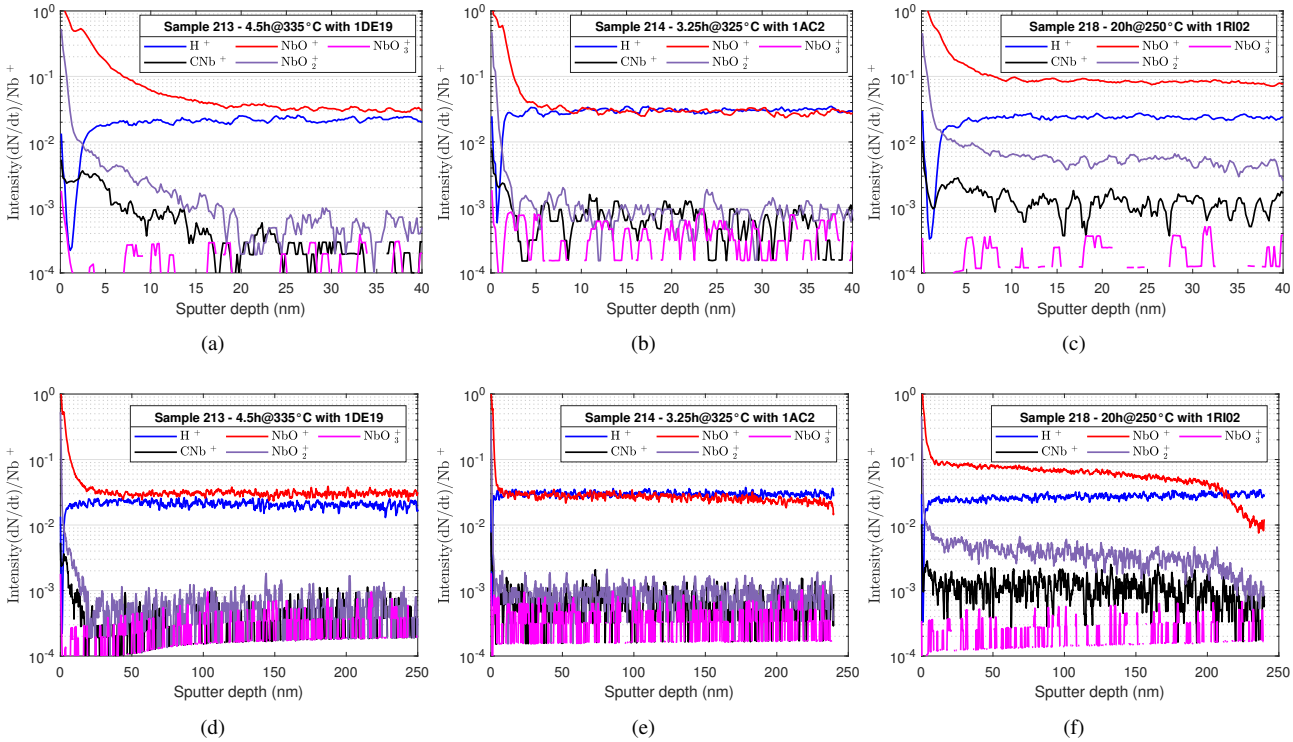

Figure 7: SIMS data of niobium samples treated with a cavity. Counts per second vs. depth are shown.

cavity preparation which makes the mid-T treatment highly cost-effective. The next immediate step is to gather more data points for different heat cycles and explore new parameters for the recipes. Furthermore, a nine-cell cavity will undergo the mid-T heat treatment in this furnace.

ACKNOWLEDGEMENTS

The accomplishment of the work described in this paper would not have been possible without the invaluable contributions of the cleanroom and AMTF teams at DESY, who played a crucial role in the preparation of the cavities and execution of the vertical tests. We would like to extend our sincere gratitude for the highly fruitful discussions with the joint DESY University of Hamburg SRF R&D team, which greatly contributed to the advancement of our research. Additionally, we would like to express our appreciation to S. Nouri Shirazi and T. Fladung from the Fraunhofer Institute for Applied Materials Research IFAM in Bremen, where the SIMS measurements have been conducted.

REFERENCES

[1] S. Posen, A. Romanenko, A. Grassellino, O. Melnychuk, and D. Sergatskov, "Ultralow surface resistance via vacuum heat treatment of superconducting radio-frequency cavities", *Phys. Rev. Appl.*, vol. 13, no. 1, p. 014024.

[2] F. He *et al.*, "Medium-temperature furnace baking of 1.3 GHz 9-cell superconducting cavities at IHEP", *Supercond. Sci. Technol.*, vol. 34, no. 9, p. 095005. doi:10.1088/1361-6668/ac1657

[3] H. Ito, H. Araki, K. Takahashi, and K. Umemori, "Influence of furnace baking on Q–E behavior of superconducting accelerating cavities", *Prog. Theor. Exp. Phys.*, vol. 2021, no. 7, p. 071G01. doi:10.1093/ptep/ptab056

[4] L. Steder *et al.*, "Medium Temperature Treatments of Superconducting Radio Frequency Cavities at DESY", in *Proc. LINAC'22*, Liverpool, UK, Aug.-Sep. 2022, pp. 840–843. doi:10.18429/JACoW-LINAC2022-THPOGE22

[5] A. Grassellino *et al.*, "Nitrogen and argon doping of niobium for superconducting radio frequency cavities: a pathway to highly efficient accelerating structures", *Supercond. Sci. Technol.*, vol. 26, p. 102001, 2013. doi:10.1088/0953-2048/26/10/102001

[6] M. Martinello *et al.*, "Effect of interstitial impurities on the field dependent microwave surface resistance of niobium", *Appl. Phys. Lett.*, vol. 109, p. 062601, 2016. doi:10.1063/1.4960801

[7] D. Gonnella *et al.*, "Industrial Cavity Production: Lessons Learned to Push the Boundaries of Nitrogen-Doping", in *Proc. SRF'19*, Dresden, Germany, Jun.-Jul. 2019, pp. 1199–1205. doi:10.18429/JACoW-SRF2019-FRCAA3

[8] L. Trelle *et al.*, "Refurbishment and Reactivation of a Niobium Retort Furnace at DESY", presented at *Proc. SRF'23*, Grand Rapids, MI, USA, Jun. 2023, paper TUPTB037, this conference.

[9] D. Reschke *et al.*, "Performance in the vertical test of the 832 nine-cell 1.3 GHz cavities for the European X-ray Free Electron Laser", *Phys. Rev. Accel. Beams*, vol. 20, p. 042004, 2017. doi:10.1103/PhysRevAccelBeams.20.042004

Content from this work may be used under the terms of the CC BY 4.0 licence (© 2023). Any distribution of this work must maintain attribution to the author(s), title of the work, publisher, and DOI

ISBN: 978-3-95450-234-9 ISSN: 2673-5504 doi:10.18429/JACoW-SRF2023-MOPMB022

[10] D. Bafia *et al.*, "New Insights on Nitrogen Doping", in *Proc. SRF'19*, Dresden, Germany, Jun.-Jul. 2019, pp. 347–354. doi:10.18429/JACoW-SRF2019-TUFUA4

[11] F. Palmer, "Surface Resistance of Superconductors - Examples from Nb-O Systems", in *Proc. SRF'87*, Lemont, IL, USA, Sep. 1987, paper SRF87C06.

[12] F. Palmer, R. Kirby, F. King, and E. Garwin, "Oxide overlayers and the superconducting rf properties of yttrium-processed high purity Nb", *Nucl. Instrum. Methods Phys. Res., Sect. A*, vol. 297, pp. 321–328, 1990. doi:10.1016/0168-9002(90)91314-2

[13] K. Kowalski, A. Bernasik, W. Singer, X. Singer, and J. Camra, "In Situ XPS Investigation of the Baking Effect on the Surface Oxide Structure Formed on Niobium Sheets Used for Superconducting RF Cavity Production", in *Proc. SRF'03*, Lübeck, Germany, Sep. 2003, paper THP09, pp. 610–613.

[14] H. Mehrer, *Diffusion in Solids. Fundamentals, Methods, Materials, Diffusion-Controlled Processes*, Springer, Berlin, Heidelberg, 2007.

[15] A. Fick, "Ueber Diffusion", *Ann. Phys.*, vol 170, pp. 59–86, 1855. doi:10.1002/andp.18551700105

[16] C. Bate, A. Ermakov, W. Hillert, D. Reschke, J. Schaffran, and M. Wenskat, "Nitrogen Infusion Sample R&D at DESY", in *Proc. IPAC'22*, Bangkok, Thailand, Jun. 2022, pp. 1219–1221. doi:10.18429/JACoW-IPAC2022-TUPOTK012

Content from this work may be used under the terms of the CC BY 4.0 licence (© 2023). Any distribution of this work must maintain attribution to the author(s), title of the work, publisher, and DOI